HBRP PUBLICATION

Research and Reviews: Journal of Mechanics and Machines
Volume 2 Issue 1

Numerical Solving the Mesoscopic Variables of LBM in Riemann Problem by Differential Quadrature Method

Mohsen Ghadyani[1*] ,Vali Enjilela[2] , Mohammad Bayat[1]
[1] *Department of Mechanics, College of Engineering, Yadegar-e-Imam Khomeini (RAH) Branch, Islamic Azad University, Tehran, Iran*
[2] *Department of Mechanical Engineering, Faculty of Mechatronics, Karaj Branch, Islamic Azad University, Karaj, Iran*
***Corresponding Author**
E-mail Id*:- m.qphd@yahoo.com*

ABSTRACT
The present study proposes a novel method for simulation of flows by a compressible LB model in order to enhance the robustness using Qadyan numerical method. The Qadyan method is a combination of semi-discrete schemes to create a system of ordinary differential equation and differential quadrature method. To illustrate the validation of the proposed method a benchmark is used to solve the mesoscopic variables of lattice Boltzmann (LB) model in Riemann problem and good agreements for inviscid flows have been obtained.

Keywords:*-LBM; Ghost field; Gibbs oscillations; Qadyan method; Mesoscopic variables; Riemann problem.*

INTRODUCTION

The original LB model by Kataoka and Tsutahara (KT) [1] uses general finite difference scheme with first-order forward in time and second-order upwinding in space. In order to obtain higher-order accuracy in the LBM, some researchers were employed the ghost field distribution functions to remove the non-physical viscous parts [2]. They also were used the conditions of the higher moment of the ghost field equilibrium distribution functions to obtain the new equilibrium distribution functions. Some numerical experiences show that the second-order finite difference scheme for calculation of space derivative, causes the Gibbs oscillations around the discontinuities [3]. Differential quadrature method (DQM) has been projected as a potential alternative to the conventional numerical solution techniques such as the finite difference and finite element methods [4]. Lattice Boltzmann method (LBM) unlike the traditional methods which solve the NavierStokes or Euler Equations directly, this method is based upon solving mesoscopic kinetic equation (Boltzmann Equation) for the particle distribution function [5]. Solution of the Riemann problem is a key ingredient of the conservative schemes to solve the Euler equations [6]. The exact solution of Riemann problem is useful in a number of ways. The solution contains the fundamental physical and mathematical character of relevant set of conservation laws subject to the initial conditions [7]. The exact Riemann problem solution is often used as a benchmarking case in assessing the performance of numerical methods [8]. Several solution techniques have been suggested in the literature to solve of initial and/or boundary problems. The differential quadrature method is one of the numerical methods. In this paper, a novel solution named Qadyan method is introduced by using of semi-discrete scheme and DQM. This numerical method confirms that macroscopic parameters (velocity, pressure, temperature and density) obtained by solving LBM reduce oscillations and satisfy the fluid dynamics equation (Euler Equation). The following parts of the paper are planned as follows. Next section describes briefy the Riemann problem and discontinuous solutions. Derivation details of the discrete velocity model are available in KT [1] so, they are not repeated here. However, for the sake of completeness, a brief description of governing equations of lattice Boltzmann model are given next. Then Qadyan numerical method is described. Results and discussion is presented in next section. Final section makes the conclusion for the present paper.

Riemann Problem and Discontinuous Solutions

In the context of Euler equations, Riemann problem is a slight generalization of the so called shock tube problem in which two stationary gases are separated by a diaphragm and the rupture of diaphragm generates a wave system. Elementary waves such as rarefaction waves, contact discontinuity waves and shock waves will be described and basic relations across these waves will be established. These relations are used to determine the complete solution of the Riemann problem. There is no closed-form solution to the Riemann problem and iterative schemes are used to arrive at the solution with a desired accuracy. In Riemann problem, the initial state of gases need not be stationary. The Riemann problem for the one-dimensional time dependent Euler equations is the initial value problem

$$W_t + F(W)_x = 0 \qquad (1)$$

with initial data W_L, W_R as bellow

$$W(x,0) = \begin{cases} W_L & : \quad x < 0.5 \\ W_R & : \quad x > 0.5 \end{cases} \qquad (2)$$

Data consists of two constant states, which in terms of initial variables are $W_L = (\rho_L, u_L, p_L)^T$ to the lleft of $x = 0.5$ and $W_R = (\rho_R, u_R, p_R)^T$ to the right of $x = 0.5$, separated by a discontinuity at $x = 0.5$. For the case in which no vacuum is present (presence of vacuum is characterized by the condition $\rho = 0$), the exact solution of Riemann problem as shown in Fig. 1 has three waves. These three waves separate our constant states which from the left to right are $(\rho_L, u_L, p_L)^T$ (data on left hand side), $(\rho_L^*, u^*, p^*)^T$, $(\rho_R^*, u^*, p^*)^T$, $(\rho_R, u_R, p_R)^T$ (data on the right hand side). The unknown region between left and right waves is the 'Star Region' which is separated into two sub-regions i.e. Star left (W_L^*) and Star right (W_R^*). The middle wave is always the contact discontinuity wave while the left and right waves may be shock or rarefaction waves.

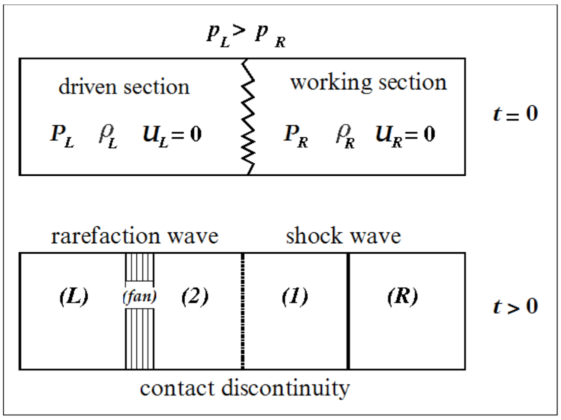

***Fig.1:**-Schematic Riemann problem and three waves*

Pressure p^* and velocity u^* do not vary across the contact discontinuity wave while the density takes two different values ρ_L^* and ρ_R^*. A solution procedure is now explained to compute the parameters in the Star region. In the following, we limit the discussion to the case in which the left wave is a rarefaction wave and the right wave is a shock wave.

The solution for pressure p^* of the Riemann problem is given by the root of algebraic equation

$$u_R - u_L + \frac{2a_L}{\gamma-1}\left((\frac{p}{p_L})^{\frac{\gamma-1}{2\gamma}} - 1 \right) + (p - p_R)\sqrt{\frac{\left(\frac{2}{(\gamma+1)\rho_R}\right)}{p + \frac{(\gamma-1)}{(\gamma+1)} p_R}} = 0 \qquad (3)$$

The unknown pressure p^* is obtained by solving the above algebraic equation which has the monotone and concave down behavior. Since behavior of the function is particularly simple and analytical expression for its derivative is also available, finding the equation roots numerically is straight forward. For example Newton-Raphson iterative procedure may be employed to find its root.

The solution for velocity u^* is given by

$$u^* = \frac{1}{2}(u_R + u_L) + \frac{1}{2}\left[(p - p_R)\sqrt{\frac{\left(\frac{2}{(\gamma+1)\rho_R}\right)}{p + \frac{(\gamma-1)}{(\gamma+1)} p_R}} - \frac{2a_L}{\gamma-1}\left((\frac{p}{p_L})^{\frac{\gamma-1}{2\gamma}} - 1 \right) \right] \qquad (4)$$

where $a_L = \sqrt{\gamma p_L / \rho_L}$ is sound speed with data on left hand side the tube. Note that The wave speed of contact discontinuity wave is u^*. In the case of rarefaction wave at left and shock wave at right, three waves from left to right are left rarefaction wave, contact discontinuity wave and right shock wave, respectively. Density ρ_L^* is obtained from the relation

$$\rho_L^* = \rho_L \left(\frac{p^*}{p_L} \right)^{1/\gamma} \qquad (5)$$

and density ρ_L^* is obtained by

$$\rho_R^* = \rho_R \left(\frac{\frac{p^*}{p_R} + \frac{\gamma-1}{\gamma+1}}{\frac{\gamma-1}{\gamma+1}\frac{p^*}{p_R} + 1} \right) \qquad (6)$$

The solution for $(\rho_{fan}, u_{fan}, p_{fan})^T$, inside the rarefaction fan is given by

$$(\rho_{fan}, u_{fan}, p_{fan})^T = \begin{vmatrix} \rho_{fan} = \rho_L \left[\frac{2}{\gamma+1} + \frac{\gamma-1}{(\gamma+1)a_L}(u_L - \frac{x}{t}) \right]^{2/(\gamma-1)} \\ u_{fan} = \frac{2}{\gamma+1}\left[a_L + \frac{\gamma-1}{2}u_L + \frac{x}{t} \right] \\ p_{fan} = p_L \left[\frac{2}{\gamma+1} + \frac{\gamma-1}{(\gamma+1)a_L}(u_L - \frac{x}{t}) \right]^{2\gamma/(\gamma-1)} \end{vmatrix} \qquad (7)$$

The rarefaction wave is enclosed by the Head and the Tail, and the speeds of these Head and Tail are given by

$$S_H = u_L - a_L \qquad (8)$$

$$S_T = u^* - a_L \left(\frac{p^*}{p_L} \right)^{(\gamma-1)/2\gamma} \qquad (9)$$

and the shock wave speed is computed using the relation

$$S_{shock} = u_R + a_R \sqrt{\frac{\gamma-1}{2\gamma}\frac{p^*}{p_R} + \frac{\gamma-1}{2\gamma}} \qquad (10)$$

The complete solution set in terms of macroscopic variables (ρ, u, p) to this case is

$$W = \begin{vmatrix} (\rho_L, u_L, p_L)^T & ; \frac{x}{t} < S_H \\ (\rho_{fan}, u_{fan}, p_{fan})^T & ; S_H < \frac{x}{t} < S_T \\ (\rho_L^*, u^*, p^*)^T & ; S_T < \frac{x}{t} < u^* \\ (\rho_R^*, u^*, p^*)^T & ; u^* < \frac{x}{t} < S_{shock} \\ (\rho_R, u_R, p_R)^T & ; \frac{x}{t} > S_{shock} \end{vmatrix} \qquad (11)$$

Governing Equations of the Lattice Boltzmann Model

The one-dimensional LB model by Kataoka and Tsutahara (KT) as considered in ref. [1] uses 5-particle discrete velocities model that is proposed for a compressible perfect gas. In this model, the equilibrium distribution function was proposed as though the compressible Euler equations are obtained. Figure 2 illustrates the sketch of this discrete-velocity-model. The model uses a lattice with 4 links that connect the center node to 4 other nodes. Here is assumed that particles are divided into three kinds that move the link with velocities 0 (the rest particle) c_1 and c_2. The amounts of c_1 and c_2 does not seem unrelated to the flow velocity u and c_2 is generally chosen $1.0 \sim 3.0$ times of c_1.

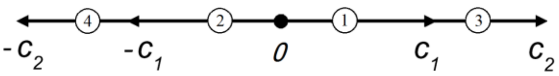

Fig.2:-*The lattice of 5-particle discrete*

velocities model

Consider the $f_i(\mathbf{x},t)$ as the distribution function at site $\mathbf{x}$ and time t, with velocity $\mathbf{v}_i$, we define the initial-value problem of the Bhatanger-Gross-Krook-type kinetic equation

$$\frac{\partial f_i}{\partial t} + \mathrm{v}_{i\alpha}\frac{\partial f_i}{\partial \mathbf{x}_\alpha} = \frac{1}{\tau}[f_i^{\mathrm{eq}}(\rho,u_\alpha,T) - f_i] \quad (12)$$

with the initial condition

$$f_i = f_i^{\mathrm{eq}}(\rho^0,u_\alpha^0,T^0) \quad \text{at} \quad t=0 \quad (13)$$

where f_i^{eq} is the discrete version of the local equilibrium distribution function; index $\alpha = 1,2$ corresponding to x, y respectively; v_i the $i-$th discrete velocity, $i = 0,...,N-1$; N is the total number of the discrete velocity; and τ is the single relaxation parameter that expresses the rate at which the local particle distribution relaxes to the local equilibrium state. This parameter determines how the momentum is transferred between the fluid particles in the collision process.

The local particle density ρ, hydrodynamic velocity u_α and temperature T are defined by

$$\rho = \sum_i f_i \quad (14)$$

$$\rho u_\alpha = \sum_i f_i \mathrm{v}_{i\alpha} \quad (15)$$

$$\rho(bRT + u_\alpha^2) = \sum_i f_i(\mathrm{v}_{i\alpha}^2 + \eta_i^2) \quad (16)$$

where R is the specific gas constant, b relates to the specific-heats ratio γ as follows, $b = 2/(\gamma-1)$ to make it flexible and η_i is another variable introduced

$$\eta_i = \begin{cases} \eta_0 & i=0 \\ 0 & i=1,...,4 \end{cases} \quad (17)$$

Perfect-gas equation relates between the temperature T and pressure p as follows

$$p = \rho RT \quad (18)$$

Considering L, ρ_0, T_0 as the reference length, density, temperature, and the reference speed $e_0 = (RT_0)^{0.5}$ the non-dimensional quantities are defined as $\hat{\mathrm{x}}_\alpha = \mathrm{x}_\alpha / L$, $\hat{t} = t/(L/e_0)$, $\hat{\mathrm{v}}_{i\alpha} = \mathrm{v}_{i\alpha}/e_0$, $\hat{f}_i = f_i/\rho_0$, $\hat{f}_i^{eq} = f_i^{eq}/\rho_0$ which lead to non-dimensional form of the evolution LB equation

$$\frac{\partial \hat{f}_i}{\partial \hat{t}} + \hat{\mathrm{v}}_{i\alpha}\frac{\partial \hat{f}_i}{\partial \hat{\mathbf{x}}_\alpha} = \frac{1}{\hat{\tau}}[\hat{f}_i^{\mathrm{eq}} - \hat{f}_i] \quad (19)$$

where parameter $\hat{\tau} = e_0\tau/L$ is the Knudsen number. The non-dimensional form is used for further discussion, but for the sake of convenience we drop the hat mark from henceforth. In the one-dimensional case, discrete velocities (Fig. 2) are defined as

$$\mathrm{v}_{i1} = \begin{cases} 0, & i=0 \\ c_1\cos[(i+1)\pi], & i=1,2 \\ c_2\cos[(i+1)\pi], & i=3,4 \end{cases} \quad (20)$$

The equilibrium distribution function f_α^{eq} is calculated in the following ways,

$$f_i^{\mathrm{eq}} = \rho(A_i + B_i \mathrm{v}_{i1} u) \quad , \quad i = 0,1,...4 \quad (21)$$

where coefficients A_i, B_i are determined by a set of reasonable requirements. The following constraints are imposed on the moments of f_i^{eq} (Here, the summation convention is not applied to the subscript i representing the kind of particles). Note that, besides the non-dimensional quantities as defined before the macroscopic variables ρ, u_α, p and T actually are in non-dimensional form regarding to reference length, density, temperature, and the reference speed ($\hat{\rho} = \rho/\rho_0$, $\hat{u}_\alpha = u_\alpha/e_0$, $\hat{T} = T/T_0$, and $\hat{p} = p/(\rho_0 e_0^2)$, also $\hat{\eta}_i = \eta_i/e_0$).

$$A_i = \begin{cases} \dfrac{b-1}{\eta_0^2}T \ , & i=0 \\ \dfrac{1}{2(c_1^2-c_2^2)}\left[-c_2^2 + \left((b-1)\dfrac{c_2^2}{\eta_0^2}+1\right)T + u^2\right], & i=1,2 \\ \dfrac{1}{2(c_2^2-c_1^2)}\left[-c_1^2 + \left((b-1)\dfrac{c_1^2}{\eta_0^2}+1\right)T + u^2\right], & i=3,4 \end{cases} \quad (22)$$

$$B_i=\begin{cases}\dfrac{-c_2^2+(b+2)T+u^2}{2c_1^2(c_1^2-c_2^2)}, & i=1,2\\ \dfrac{-c_1^2+(b+2)T+u^2}{2c_2^2(c_2^2-c_1^2)}, & i=3,4\end{cases} \tag{23}$$

The complete solution set for the distribution functions is

$$f_i^{eq}=\begin{cases}A_i\rho_L+B_i\rho u_L \mathrm{v}_{i1} & ;\ \frac{x}{t}<S_H\\ A_i\rho_{fan}+B_i\rho_{fan}u_{fan}\mathrm{v}_{i1} & ;\ S_H<\frac{x}{t}<S_T\\ A_i\rho_L^*+B_i\rho_L^*u^*\mathrm{v}_{i1} & ;\ S_T<\frac{x}{t}<u^*\\ A_i\rho_R^*+B_i\rho_R^*u^*\mathrm{v}_{i1} & ;\ u^*<\frac{x}{t}<S_{shock}\\ A_i\rho_R+B_i\rho_R u_R\mathrm{v}_{i1} & ;\ \frac{x}{t}>S_{shock}\end{cases} \tag{24}$$

In the lattice Boltzmann model, if we assume that the gas is near-vacuum condition, the collision does not occur in the range of the mean free path. Therefore, we define the vacuum as a region where there is no particle collisions in the interval of t to $t+\Delta t$. On the other hand, if we delay the time, i.e. increase the collision time, collisions will surely occur. Thus, the phrase of $\tau\to\infty$ corresponds to $f\to f^{eq}$ and in the numerical solutions when $\Delta t\to 0$ at time-marching $f_i(\mathbf{x},t)$ can be approximated by $f_i^{eq}(\mathbf{x},t)$. Therefore, the following moments of $f_i^{eq}(\mathbf{x},t)$ can be used to obtain the macroscopic variables ρ,u,T.

$$\rho=\sum_i f_i^{eq} \tag{25}$$

$$\rho u=\sum_i f_i^{eq}\mathrm{v}_{i1} \tag{26}$$

$$\rho(bRT+u^2)=\sum_i f_i^{eq}(\mathrm{v}_{i1}^2+\eta_i^2) \tag{27}$$

Qadyan Numerical Method

To reach second-order accuracy in the LBM, some researchers were employed the ghost field distribution functions. However this method is not discussed here. Although KT model uses general finite difference scheme with first-order forward in time and second-order upwinding in space, the numerical experiences showed the second-order finite difference scheme for space derivative calculation causes the Gibbs oscillations around the discontinuities. Here without going into the mathematical basis of the differential quadrature method, we introduce Qadyan method. This method is obtained by semi-discrete schemes. It means that one solves the system of ordinary differential equations:

$$f_i(\mathrm{x},t+\Delta t)=f_i(\mathrm{x},t)-\Delta t\ \mathrm{v}_{i\alpha}\frac{\partial f_i}{\partial \mathbf{x}_\alpha}-\frac{\Delta t}{\tau}[f_i(\mathrm{x},t)-f_i^{eq}(\mathrm{x},t)] \tag{28}$$

Here the space derivative $\dfrac{\partial f_i}{\partial \mathbf{x}_\alpha}$ approximates by DQ method as follows.

In the case of $\mathrm{v}_{i1}=c_1>0$, or $\mathrm{v}_{i1}=c_2>0$

$$\frac{\partial(f_i)}{\partial \mathbf{x}_\alpha}=\frac{1}{\Delta \mathbf{x}_\alpha}\begin{bmatrix}\frac{-11}{6} & 3 & \frac{-3}{2} & \frac{1}{3} & 0 & 0 & \cdots & 0 & 0 & 0\\ \frac{-1}{3} & \frac{-1}{2} & 1 & \frac{-1}{6} & 0 & 0 & \cdots & 0 & 0 & 0\\ \frac{1}{6} & -1 & \frac{1}{2} & \frac{1}{3} & 0 & 0 & \cdots & 0 & 0 & 0\\ 0 & \frac{1}{6} & -1 & \frac{1}{2} & \frac{1}{3} & 0 & \cdots & 0 & 0 & 0\\ 0 & 0 & \frac{1}{6} & -1 & \frac{1}{2} & \frac{1}{3} & \cdots & 0 & 0 & 0\\ 0 & 0 & 0 & \frac{1}{6} & -1 & \frac{1}{2} & \cdots & 0 & 0 & 0\\ \vdots & \vdots & \vdots & \vdots & \vdots & \vdots & \vdots & \vdots & \vdots & \vdots\\ 0 & 0 & 0 & 0 & 0 & \frac{1}{6} & -1 & \frac{1}{2} & \frac{1}{3} & 0\\ 0 & 0 & 0 & 0 & 0 & 0 & \frac{1}{6} & -1 & \frac{1}{2} & \frac{1}{3}\\ 0 & 0 & 0 & 0 & 0 & 0 & \frac{-1}{3} & \frac{3}{2} & -3 & \frac{11}{6}\end{bmatrix}\begin{Bmatrix}(f_i)_1\\(f_i)_2\\(f_i)_3\\(f_i)_4\\(f_i)_5\\(f_i)_6\\ \vdots\\(f_i)_{N-2}\\(f_i)_{N-1}\\(f_i)_N\end{Bmatrix} \tag{29}$$

In the case of $\mathrm{v}_{i1} = -c_1 < 0$, or $\mathrm{v}_{i1} = -c_2 < 0$

$$\frac{\partial (f_i)}{\partial \mathbf{x}_\alpha} = \frac{1}{\Delta \mathbf{x}_\alpha}\begin{bmatrix} \frac{-11}{6} & 3 & \frac{-3}{2} & \frac{1}{3} & 0 & 0 & \cdots & 0 & 0 & 0 \\ \frac{-1}{3} & \frac{-1}{2} & 1 & \frac{-1}{6} & 0 & 0 & \cdots & 0 & 0 & 0 \\ 0 & \frac{-1}{3} & \frac{-1}{2} & 1 & \frac{-1}{6} & 0 & \cdots & 0 & 0 & 0 \\ 0 & 0 & \frac{-1}{3} & \frac{-1}{2} & 1 & \frac{-1}{6} & \cdots & 0 & 0 & 0 \\ 0 & 0 & 0 & \frac{-1}{3} & \frac{-1}{2} & 1 & \cdots & 0 & 0 & 0 \\ 0 & 0 & 0 & 0 & \frac{-1}{3} & \frac{-1}{2} & \cdots & 0 & 0 & 0 \\ \vdots & \vdots & \vdots & \vdots & \vdots & \vdots & \vdots & \vdots & \vdots & \vdots \\ 0 & 0 & 0 & 0 & 0 & 0 & \frac{-1}{3} & \frac{-1}{2} & 1 & \frac{-1}{6} \\ 0 & 0 & 0 & 0 & 0 & 0 & \frac{1}{6} & -1 & \frac{1}{2} & \frac{1}{3} \\ 0 & 0 & 0 & 0 & 0 & 0 & \frac{-1}{3} & \frac{3}{2} & \frac{-3}{h} & \frac{11}{6} \end{bmatrix} \left\{ \begin{matrix} (f_i)_1 \\ (f_i)_2 \\ (f_i)_3 \\ (f_i)_4 \\ (f_i)_5 \\ (f_i)_6 \\ \vdots \\ (f_i)_{N-2} \\ (f_i)_{N-1} \\ (f_i)_N \end{matrix} \right\} \tag{30}$$

RESULTS AND DISCUSSION

A benchmark is used to validate the proposed method. The problem is the solution of the well-known test, namely Sod's shock-tube problem [9] which consist of initial data as

$$\begin{aligned} (\rho, u, p)\big|_L &= (1,\ 0,\ 1), & x < 0.5 \\ (\rho, u, p)\big|_R &= (0.125,\ 0,\ 0.1), & x > 0.5 \end{aligned} \tag{31}$$

The shock Mach number of the Sod's test is 1.656 (which is defined as the speed of shock divided by the speed of sound ahead of the shock). All the above phenomena consist of rarefaction wave, contact discontinuity, and shock wave are included in the Sod's problem. Therefore this test is the proper one in order to fulfill results in the combined phenomena problem. The comparison between the numerical results and the analytic results for distribution functions are plotted in figures 3 and 4. The grids size used in the simulation is $\Delta x = 0.02$, time step $\Delta t = 0.5 \times 10^{-4}$ and the results are plotted after $t = 0.15$ second past initial state. The parameters used in the simulation are $c_1 = 1$, $c_2 = 3$, and $\eta_0 = 2$. The solutions are obtained with lattice size 500 after 3000 time-steps.

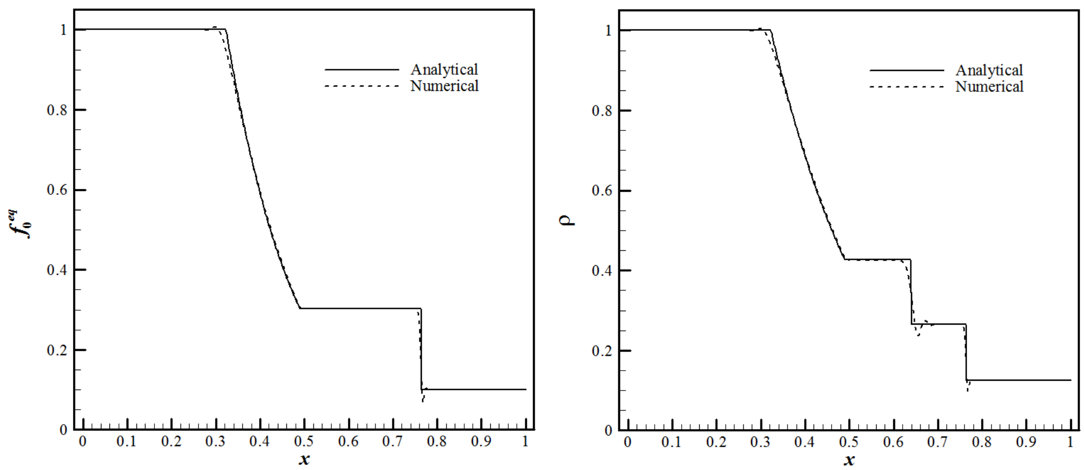

***Fig.3:**-The comparison between analytical and numerical results of f_0^{eq} and ρ with $c_1 = 1, c_2 = 3$.*

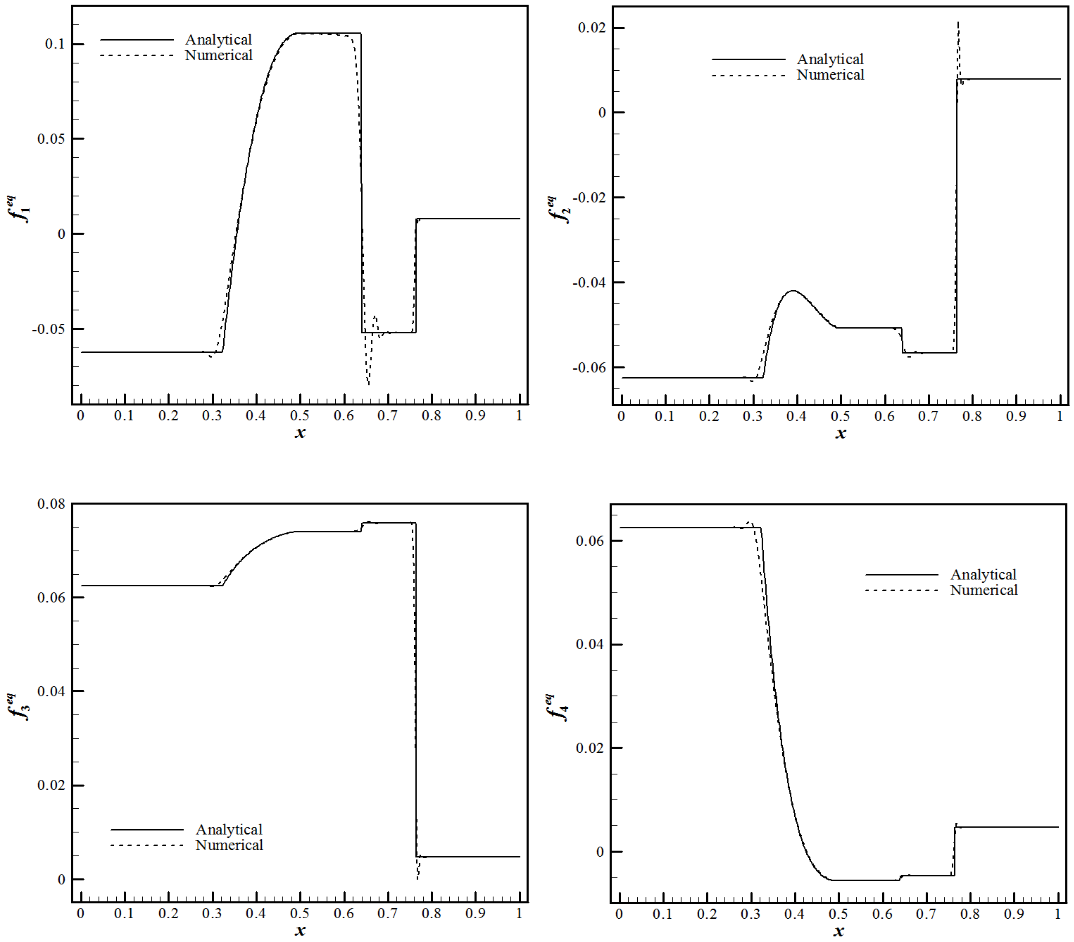

Fig.4:-*The comparison between analytical and numerical results of* f_1^{eq} *to* f_4^{eq} *with* $c_1 = 1, c_2 = 3.$

The comparison between the numerical results and the analytic results for distribution functions are plotted in Figures 5 and 6. All the parameters used in the simulation are same unless $c_1 = 2, c_2 = 6$. The solutions are also obtained with lattice size 500 after 3000 time steps.

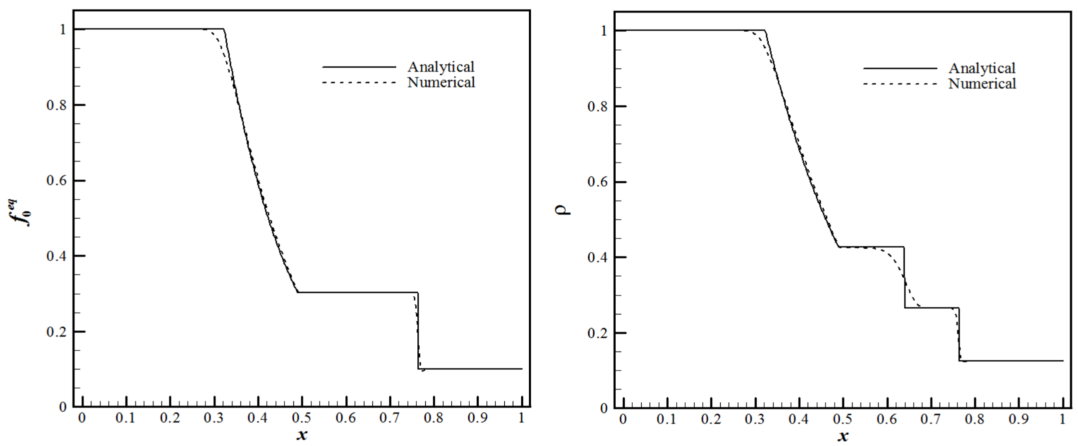

Fig.5:- *The comparison between analytical and numerical results of* f_0^{eq} *and* ρ *with* $c_1 = 2, c_2 = 6.$

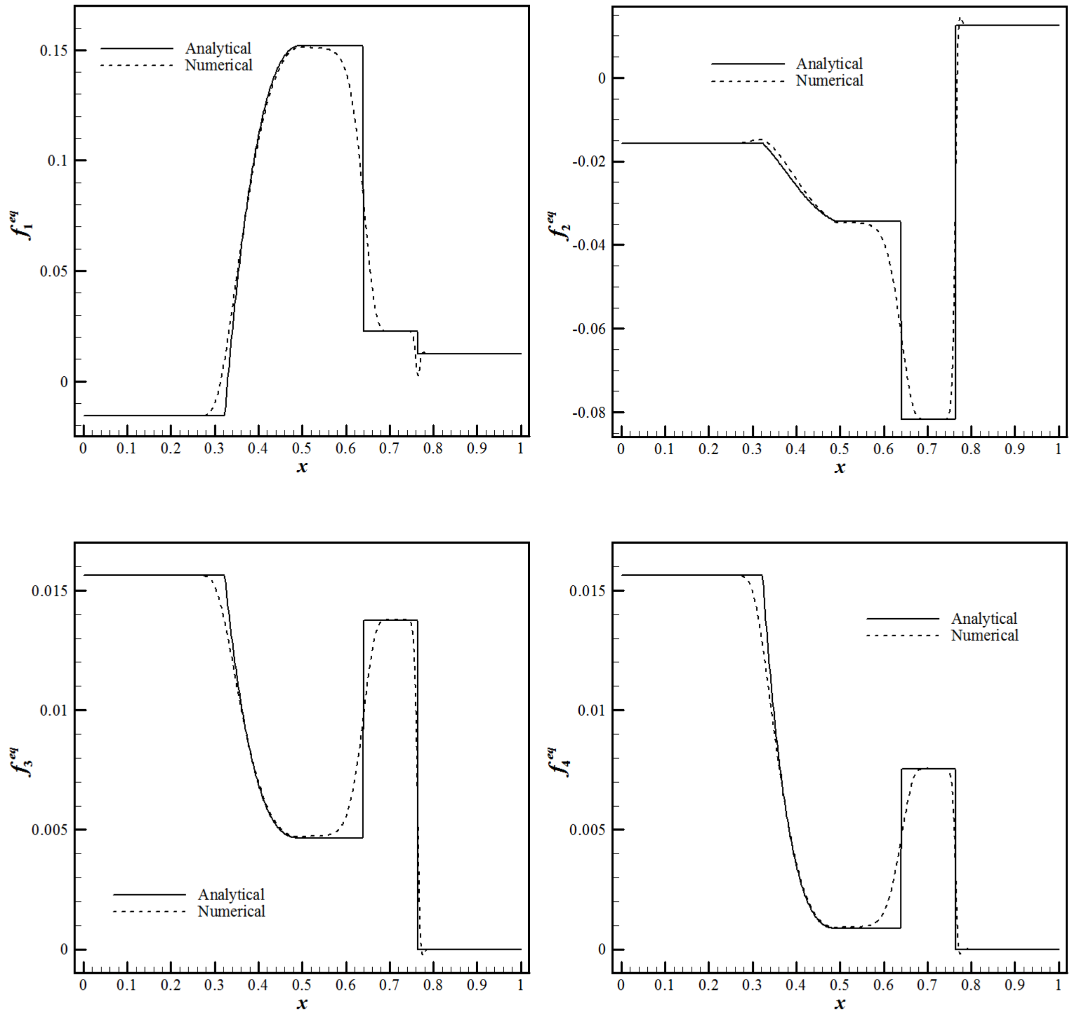

***Fig.6:-**The comparison between analytical and numerical results of f_1^{eq} to f_4^{eq} with* $c_1 = 2, c_2 = 6.$

CONCLUSIONS

In this paper, we report the numerical solving of the mesoscopic variables of LBM and compare analytic solution by Qadyan method. The Euler equation's solutions may contain discontinuity waves such as contact discontinuity and shock waves. Some stringent requirements are posed by such discontinuities on the numerical schemes or the mathematical formulation of equations to solve the governing formulations. The non–conservative equations may fail at discontinuities and give wrong shock strength or shock speeds. It has been established that conservative numerical methods do converge to the weak solution of the conservation law. The validity of the procedure has been investigated for Sod's Shock-Tube Problem and good agreements have been obtained. The amounts of particle velocities c_1 and c_2 in LB model does not seem unrelated to the flow velocity u or othe macroscopic flow variables and amounts of them change the mesoscopic variables.

ACKNOWLEDGMENTS

This work was supported, in part, by the Islamic Azad university of Yadegar-e-Imam Khomeini (RAH) Branch, and by the Karaj Branch of the Islamic Azad University. The authors pay respect and their appreciation to all supporters of this research.

REFERENCES

1. Kataoka T., Tsutahara M. Lattice *Boltzmann method for the compressible Euler equations*. Physical Review. 2004.69:1–14p.
2. Zhang J,Yan GW., Shi X., Dong Y. *A lattice Boltzmann model for the compressible Euler equations with second-order accuracy*. Int. J. Numer. Meth. Fluids.2009.60:95–117p.
3. Ghadyani M., Esfahanian V., Taeibi-Rahni M. *The use of shock-detecting sensor to improve the stability of lattice Boltzmann model for high Mach number flows*. International Journal of Modern Physics C.2015.26 (1).
4. Charles W. Bert, Moinuddin Malik. *Differential quadrature method in computational mechanics: A review*. Appl. Mech. Rev. 1996.49(1).
5. Ghadyani M., Esfahanian V. *A more robust compressible lattice Boltzmann model by using the numerical filters*. Journal of Mechanics. 2014.30:515-525p.
6. Toro E. F. *Riemann solvers and numerical methods for fluid dynamics*. 2nd Edition, Springer Publication, 1999.
7. Anderson J.D. *Modern compressible flow*. 3rd Edition, Mc. Graw Hill Publications, 2003.
8. Esfahanian V., Ghadyani M.. *Improvement of the instability of compressible lattice Boltzmann model by shock-detecting sensor*. Journal of Mechanical Science and Technology. 2015.29(5):1981-1991p.
9. Sod, G. A. *A Survey of several finite difference methods for systems of nonlinear hyperbolic conservation laws*. Journal of Computational Physics. 1978.27 (1):1–31p.